

ACOUSTIC TOMOGRAPHY METHOD FOR MEASURING TEMPERATURE AND WIND VELOCITY

Ivana Jovanović[†], Luciano Sbaiz[†] and Martin Vetterli^{†§}

[†] School of Computer and Communication Sciences

Ecole Polytechnique Fédérale de Lausanne (EPFL), CH-1015 Lausanne, Switzerland

[§] Department of Electrical Engineering and Computer Sciences

University of California at Berkeley (UCB), Berkeley, CA 94720, USA

email: {ivana.jovanovic, luciano.sbaiz, martin.vetterli}@epfl.ch

ABSTRACT

We consider the problem of reconstructing superimposed temperature and wind flow fields from acoustic measurements. A new technique based solely on acoustic waves propagation is presented. In contrast to the usual straight ray assumption, a bent ray model is considered in order to achieve higher accuracy. Under this assumption, we propose an iterative reconstruction algorithm that allows to entirely recover the considered fields. It alternates between estimating the fields of interest and the corresponding acoustic ray trajectories. Simulation results confirm the effectiveness and fast convergence of our scheme.

1. INTRODUCTION

Tomography methods aim at recovering an unknown multi-dimensional field based on the interactions between the considered medium and radiations emitted by measuring devices. They offer an attractive alternative to classical methods employed in sensor networks, since they allow non-invasive measurements with a significantly smaller number of sensing devices. In fact, the information acquired by processing signals transmitted and received at multiple locations allows to acquire a global knowledge about the measured field. This is in sharp contrast to the one-sensor one-measurement setup provided by traditional sensor networks.

In this work, we focus on the use of acoustic tomography for measuring temperature and wind flow fields. The strong dependance of sound propagation on these quantities offers promising perspectives for accurate estimation of the entire fields. It thus stands as a good candidate to replace some of today's expensive meteorological techniques using sodar or lidar.

The estimation of temperature fields is a scalar tomography problem in the sense that it amounts to recover a scalar function from line-integral measurements. Under quite general conditions, acoustic time of flight data typically provide the information needed to solve this problem by means of the Radon transform. The reconstruction of wind flow fields, however, deals with vector tomography for which acoustic techniques are only partially envisioned in practice. The main reason lies in the existence of "invisible fields" for time of flight measurements. This fact was first noticed by Johnson *et al.* [1]

This research was supported by the National Competence Center in Research on Mobile Information and Communication Systems (NCCR-MICS, <http://www.mics.org>), a center supported by the Swiss National Science Foundation under grant number 5005-67322.

in their early study of acoustic time of flight data. Later, Braun and Hauck [2] pointed out that time of flight measurements only allow to reconstruct the source-free component of the vector field. They formulated conditions enabling full vector field recovery and proposed to estimate the remaining (curl-free) component using an additional line-integral measurement. The two line integrals, referred to as *longitudinal* and *transversal* interactions, actually correspond to the integration of the tangential and normal component of the vector field along the propagation path. The method they proposed to measure the transversal component is based on an optical Schlieren technique that is only applicable in rather specialized scenarios [2].

Motivated by the practical need of full vector field reconstruction, we propose in this paper a new method for measuring the transversal component based solely on acoustic wave measurements. We show that the transversal interaction can be inferred from the angle of arrival of the sound waves. Based on time of flight and angle of arrival measurements, we then propose an algorithm that alternates between estimating the ray trajectories and the fields of interest. High reconstruction accuracy is achieved by replacing the commonly assumed straight-ray model by a bent-ray model [3]. We observe that the procedure converges even in cases where the ray paths differ considerably from straight lines. To our knowledge, the joint estimation of ray trajectories, temperature and wind flow fields has never been addressed before.

2. THEORY AND FUNDAMENTALS OF THE METHOD

2.1. Scalar and Vector Tomography

Classical tomography methods, referred to as *scalar field tomography*, assume that every point of the field is characterized by a scalar. In this case, the field can be determined from line-integral measurements along multiple directions by applying an inverse Radon transform. The ability to reconstruct a scalar function using tomography techniques has resulted in a wealth of applications in many disciplines. Examples are x-ray tomography in biomedicine, acoustic tomography in oceanography and seismic tomography in geophysics. A number of other applications has raised the need for similar methods in tomographic reconstruction of vector fields. The basic idea, proposed in [2], is to treat each component of the original *vector field tomography* problem using a scalar field tomography method. In two-dimensional acoustic tomography, a natural choice for the corresponding line-integral measurements are the so-called *longitudinal* and *transversal* interactions, denoted respectively by l_{Γ} and

t_Γ . More precisely, for any vector function \mathbf{f} defined on the region of interest, l_Γ and t_Γ are given by

$$\begin{aligned} l_\Gamma &= \int_\Gamma \mathbf{f} \cdot \mathbf{t} \, ds, \\ t_\Gamma &= \int_\Gamma \mathbf{f} \cdot \mathbf{m} \, ds, \end{aligned} \quad (1)$$

where Γ is the ray path, \mathbf{t} the unit vector tangent to Γ and \mathbf{m} the unit vector normal to Γ (see Fig. 1(a)). If \mathbf{f} represents a wind velocity, then the integral l_Γ typically arises in acoustic time of flight measurements. Unfortunately, the second integral t_Γ cannot be computed from time of flights and has never been considered in flow reconstruction problems using acoustic tomography.

2.2. Geometrical Acoustic

The main advantages offered by the ray theory of sound wave propagation are its simplicity and the clarity it offers in representing the underlying physical phenomena. One of the principal tasks is to obtain the ray path along which the energy of a sound wave is propagated. In previous research on acoustic tomography, a straight-ray model is usually assumed. This seriously limits the quality of the reconstruction since it does not account for the deformation of the wave trajectory. In this paper, we propose to use a bent-ray model to provide a more precise estimation of the vector fields and to extend the applicability of the method to strong fields. In the following, we will use the equations derived by Ostashev [4] for the ray path in an inhomogeneous moving medium

$$\begin{aligned} \dot{\mathbf{x}}(s) &= c \frac{\mathbf{b}}{\|\mathbf{b}\|} + \mathbf{v}, \\ \dot{\mathbf{b}}(s) &= -\frac{c_0 \nabla c}{c} - \mathbf{J}_v \mathbf{b} + \frac{\mathbf{b} \cdot \mathbf{v} \nabla c}{c}, \end{aligned} \quad (2)$$

where the sound speed c is written as $c = c_0 + \Delta c$ for some average sound speed c_0 and variation Δc . In the above equations, s and \mathbf{x} are respectively the arc length and the space coordinate measured along Γ , \mathbf{J}_v is the Jacobian matrix of the wind field \mathbf{v} , and \mathbf{b} is the vector with norm $\|\mathbf{b}\| = c_0 / (c + \mathbf{n} \cdot \mathbf{v})$ and direction $\mathbf{n} = \mathbf{b} / \|\mathbf{b}\|$ normal to the wave front. In order to compute the ray path, we use the initial conditions

$$\mathbf{x}(0) = \mathbf{x}_T \quad \text{and} \quad \mathbf{b}(0) = \frac{c_0}{c(0) + \mathbf{n}(0) \cdot \mathbf{v}(0)} \mathbf{n}(0). \quad (3)$$

The starting point corresponds to the position \mathbf{x}_T of the transmitter and the initial ray direction $\mathbf{n}(0) = (\cos \theta, \sin \theta)^T$ is chosen such that the ray reaches the receiver. The angle θ is shown in Fig. 1(a).

2.3. Temperature and Wind Reconstruction

In dry air, the temperature T can be inferred from the speed of sound through the relation

$$c = \sqrt{\gamma R T}, \quad (4)$$

where R is the gas constant and $\gamma = 1.4$. We will thus concentrate on estimating c in the rest of the discussion. The total speed \mathbf{u} , also referred to as *group velocity*, is given by

$$\mathbf{u} = c \mathbf{n} + \mathbf{v} = (c_0 + \Delta c) \mathbf{n} + \mathbf{v}. \quad (5)$$

In this work, we wish to reconstruct both the temperature (scalar) and wind (vector) field. To this end, we define the longitudinal interaction of a joint vector and scalar field as

$$l_\Gamma = \int_\Gamma (\Delta c \mathbf{n} + \mathbf{v}) \cdot \mathbf{t} \, ds. \quad (6)$$

The time of flight t_{ij} of a sound ray from transmitter i to the receiver j along the trajectory Γ_{ij} can be expressed using a simple Taylor expansion as

$$\begin{aligned} t_{ij} &= \int_{\Gamma_{ij}} \frac{1}{\mathbf{u} \cdot \mathbf{t}} \, ds \\ &\simeq \int_{\Gamma_{ij}} \frac{1}{c_0 \mathbf{n} \cdot \mathbf{t}} \, ds - \int_{\Gamma_{ij}} \frac{(\Delta c \mathbf{n} + \mathbf{v}) \cdot \mathbf{t}}{(c_0 \mathbf{n} \cdot \mathbf{t})^2} \, ds \\ &= \int_{\Gamma_{ij}} \frac{1}{c_0 \mathbf{n} \cdot \mathbf{t}} \, ds - \frac{F(\mathbf{x}_{T_i}, \mathbf{x}_{R_j}, \mathbf{v}, \Delta c)}{c_0^2} l_{\Gamma_{ij}} \end{aligned} \quad (7)$$

where \mathbf{x}_{T_i} and \mathbf{x}_{R_j} are the position of transmitter i and receiver j , respectively. The term $F(\mathbf{x}_{T_i}, \mathbf{x}_{R_j}, \mathbf{v}, \Delta c)$ is a correction factor needed to replace $(c_0 \mathbf{n} \cdot \mathbf{t})$ by c_0 . Typically, both Δc and \mathbf{v} are small, hence $F(\mathbf{x}_{T_i}, \mathbf{x}_{R_j}, \mathbf{v}, \Delta c) \simeq 1$. The longitudinal interaction $l_{\Gamma_{ij}}$ can thus be estimated from (7) using time of flight measurements.

The transversal interaction of a joint vector and scalar field can be defined similarly to (6) as

$$t_\Gamma = \int_\Gamma (\Delta c \mathbf{n} + \mathbf{v}) \cdot \mathbf{m} \, ds. \quad (8)$$

Since the total speed along the trajectory is tangent to the trajectory, it holds that $(c_0 \mathbf{n} + \Delta c \mathbf{n} + \mathbf{v}) \cdot \mathbf{m} = 0$. The transversal component for trajectory Γ_{ij} can thus be written as

$$\begin{aligned} t_{\Gamma_{ij}} &= - \int_{\Gamma_{ij}} c_0 \mathbf{n} \cdot \mathbf{m} \, ds \\ &= -c_0 \int_{\Gamma_{ij}} \begin{pmatrix} \cos \theta_{ij} \\ \sin \theta_{ij} \end{pmatrix} \cdot (\mathbf{t} \times \mathbf{e}_z) \, ds \\ &\simeq c_0 (-\cos \theta_{ij} (y_{R_j} - y_{T_i}) + \sin \theta_{ij} (x_{R_j} - x_{T_i})), \end{aligned} \quad (9)$$

where in the second equality, we use the fact that $\mathbf{m} = \mathbf{t} \times \mathbf{e}_z$, \mathbf{e}_z being the unit vector parallel to the z axis. We also assume \mathbf{n} to be constant, which is to say that the temperature and wind fields are uniform. This strong assumption is however relaxed in the practical algorithm described in Section 3, since we are computing the transversal component of the error field and only the *difference* between \mathbf{n} and its current estimate $\hat{\mathbf{n}}$ is assumed to be constant. Equation (9) shows that the transversal interaction can be approximately computed with the angle of arrival θ_{ij} of the sound wave and the exact position of the transmitter and the receiver. Moreover, the feedback scheme ensures that the approximation error does not influence the result but only the number of iterations needed for convergence.

2.4. Measuring the Angle of Arrival

We propose two methods for measuring the angle of arrival of the sound wave. If we ensure that around the receiver we have $\mathbf{v} = \mathbf{0}$, e.g. by putting some wind shields, then the angle θ is equal to the angle of arrival of the sound wave.

2.4.1. Acoustic dipole

An acoustic dipole consists of two sensors (microphones, hydrophones, etc.) placed at a certain distance on the measurement plane. If the curvature of the received sound wave can be neglected (far field assumption), the time difference of arrival of the test signal at the two sensors is proportional to the distance between the sensors and the cosine of the angle of arrival. Therefore, the angle of arrival can be estimated from this quantity and the distance between the sensor can be adjusted to obtain a certain sensitivity.

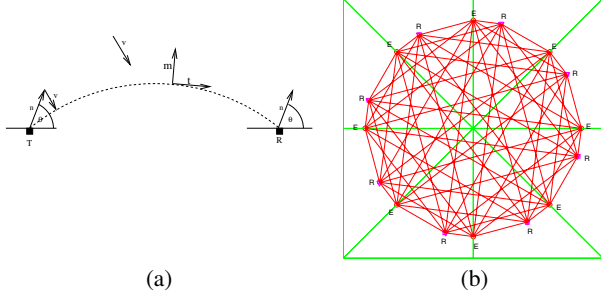


Fig. 1. (a) An example of the ray trajectory with the vectors \mathbf{n} , \mathbf{t} and \mathbf{m} ; (b) The region of interest is surrounded by 8 transmitters and 8 receivers.

2.4.2. Blumlein microphone

This method is based on the use of two directional sensors. The principle is very well known in the field of audio stereo recording. It employs two sensors which are sensitive to acoustic pressure on a diaphragm. The pressure changes proportionally to the cosine of the angle of arrival. The measured amplitude is thus related to the angle of arrival.

3. ITERATIVE ALGORITHM

We consider a certain region surrounded by emitters and receivers, as show on Fig. 1(b). Each transmitter is sending a signal to all receivers. We measure the time of flight and the angle of arrival of the sound wave front. In order to implement the reconstruction algorithm, we cover the region of interest with tessellation cells, as it is done in finite element methods. Every value inside the cells is approximated by a linear combination of the nodal point values

$$f(\mathbf{x}) = \sum_{i=1}^N f_i \alpha_i(\mathbf{x}), \quad (10)$$

where $f(\mathbf{x})$ can be any component of the wind field, v_x , v_y or temperature variation related to Δc . The value f_i is the corresponding value at node i . For example, one can cover the domain with a tiling of triangles. In such a case $N = 3$ and the function $\alpha_i(\mathbf{x})$ is the two-dimensional spline of order 1. Equation (10) allows to write the set of interactions as a linear combination of the unknown components v_x , v_y and Δc

$$\begin{bmatrix} \mathbf{M}_1 \\ \mathbf{M}_t \end{bmatrix} \cdot \begin{bmatrix} \mathbf{v}_x \\ \mathbf{v}_y \\ \Delta c \end{bmatrix} = \begin{bmatrix} \mathbf{I}_\Gamma \\ \mathbf{t}_\Gamma \end{bmatrix} \quad (11)$$

The previous equation is an approximation of (6) and (8), where the integrals are replaced with sums, and the components $\mathbf{v}_x(\mathbf{x})$, $\mathbf{v}_y(\mathbf{x})$ and $\Delta c(\mathbf{x})$ are modelled using (10). The matrixes \mathbf{M}_1 and \mathbf{M}_t are computed from (6), (8) and (10). This system allows computing the temperature and wind flow, once the trajectories are known.

In our algorithm, iterations alternate between estimating the temperature and the wind field and computing the trajectories. The difference between the estimated and true longitudinal and transversal interactions is then used to compute the new speed variation and wind field estimate

$$\begin{aligned} \Delta c^{(l+1)} &= \Delta c^{(l)} + \Delta c_e^{(l)}, \\ \mathbf{v}^{(l+1)} &= \mathbf{v}^{(l)} + \mathbf{v}_e^{(l)}, \end{aligned} \quad (12)$$

where l is the iteration number and $\Delta c_e^{(l)}$ and $\mathbf{v}_e^{(l)}$ are the new updates.

In the following we summarize the algorithmic steps:

1. Set $\mathbf{v}^{(0)} = \mathbf{0}$, $\Delta c^{(0)} = 0$, $l = 0$.
2. Compute trajectories Γ_{ij} from (2), using the current estimates $\hat{\mathbf{v}}^{(l)}$ and $\Delta c^{(l)}$, and set $\hat{\theta}^{(l)}$ such that the trajectory reaches the receiver.
3. Calculate the estimated time of flight:

$$\hat{t}_{ij} = \int_{\hat{\Gamma}_{ij}} \frac{1}{\hat{\mathbf{u}}^{(l)} \cdot \mathbf{t}} ds. \quad (13)$$

4. Compute estimation of longitudinal interactions of the error field:

$$\hat{I}_{\Gamma_{ij}}(\mathbf{v}_e, \Delta c_e) = (t_{ij} - \hat{t}_{ij}) \frac{c_0^2}{\hat{F}^{(l)}(\mathbf{x}_T, \mathbf{x}_R, \hat{\mathbf{v}}^{(l)}, \Delta \hat{c}^{(l)}), \quad (14)$$

with

$$\hat{F}^{(l)}(\mathbf{x}_T, \mathbf{x}_R, \hat{\mathbf{v}}^{(l)}, \Delta \hat{c}^{(l)}) = \frac{c_0^2}{S(\hat{\Gamma}_{ij})} \int_{\hat{\Gamma}_{ij}} \frac{1}{(c_0 \hat{\mathbf{n}}^{(l)} \hat{\mathbf{t}}^{(l)})^2} ds, \quad (15)$$

where $S(\hat{\Gamma}_{ij})$ is the length of $\hat{\Gamma}_{ij}$.

5. Estimate the transversal interaction of the error field, as:

$$\begin{aligned} \hat{t}_{\Gamma_{ij}}(\mathbf{v}_e, \Delta c_e) &= t_{\Gamma_{ij}}(\mathbf{v}, \Delta c) - \hat{t}_{\Gamma_{ij}}(\hat{\mathbf{v}}^{(l)}, \Delta \hat{c}^{(l)}) \\ &= c_0((\sin \theta - \sin \hat{\theta}^{(l)})(y_R - y_T) \\ &\quad + (\cos \theta - \cos \hat{\theta}^{(l)})(x_R - x_T)). \end{aligned} \quad (16)$$

6. Build the system (11) using (10) and the current estimation of trajectories $\hat{\Gamma}^{(l)}$.
7. Solve the system and compute errors $\hat{\mathbf{v}}_e^{(l)}$ and $\Delta \hat{c}_e^{(l)}$.
8. Update the current version of the wind flow and the speed variation as shown in (12).
9. Set $l = l + 1$ and go to step 2.

4. CRAMER-RAO LOWER BOUND FOR THE TIME OF FLIGHT MEASUREMENTS

Several technical aspects influence the performance of the tomographic reconstruction. The most important are:

1. The measurement accuracy of the distance between transmitter and receiver;
2. The accuracy of the travel-time measurements and the angle measurements;
3. The coverage of the area by sound rays and the ability of the technique to resolve different acoustic paths.

Even though the accuracy depends on many factors, in order to get an intuition about the errors, we show the Cramer-Rao lower bound on time of flight estimation. Moreover, in the case of using acoustic dipole for the angle estimate, we compute the angle of arrival from the difference of the two time of flight measurements.

Suppose we want to estimate the time of flight t_{ij} of an acoustic signal embedded in white Gaussian noise. We assume that the signal autospectrum is two sided and extends from f_1 to f_2 Hz (and also from $-f_1$ to $-f_2$ Hz). Assume that the spectral density is

$S_0/2[W/Hz]$, while the spectral density of the noise is N_0 . Therefore, the signal power is $S = S_0(f_2 - f_1)$, and the noise power is $N = N_0(f_2 - f_1)$. If we compute the Cramer-Rao lower bound for the above case of signals in white gaussian noise [5], we obtain:

$$\sigma_t^2 \geq \frac{3}{8\pi^2 T_o} \frac{1}{SNR} \frac{1}{(f_2^3 - f_1^3)} \quad (17)$$

where σ_t^2 is the variance of time of flight, $SNR = S/N$, and T_o is the observation time. In terms of bandwidth W and central frequency f_0 , taking that $f_1 = f_0 - W/2$ and $f_2 = f_0 + W/2$, the variance can be written as:

$$\sigma_t^2 = \left(\frac{1}{8\pi^2} \right) \frac{1}{SNR} \frac{1}{T_o W} \frac{1}{f_0^2} \frac{1}{(1 + W^2/12f_0^2)}. \quad (18)$$

If we change the parameters in (18) with the one that we use in our simulations, $T_o = 1ms$, $f_0 = 40kHz$, $W = 4kHz$ and for the two cases of SNR, we have

$$\begin{aligned} SNR = 50dB &\longrightarrow \sigma_t \simeq 4.4ns, \\ SNR = 30dB &\longrightarrow \sigma_t \simeq 44ns. \end{aligned} \quad (19)$$

To convert this accuracy to the temperature and wind estimation accuracy, we consider the worst case of wind speed $v = 50m/s$, and we obtain:

$$\begin{aligned} SNR = 50dB &\longrightarrow \Delta v = 10^{-5}m/s, \Delta T = 0.001K, \\ SNR = 30dB &\longrightarrow \Delta v = 0.3 \cdot 10^{-4}m/s, \Delta T = 0.01K. \end{aligned} \quad (20)$$

This is a promising result, since even for a very low signal to noise ratio we still can have a very high estimation accuracy.

5. SIMULATION RESULTS

In this section, we present the simulation results for the setup shown on Fig. 1(b). The true sound field variation Δc is given on Fig. 2. On Fig. 3, we plot the reconstruction error of $\Delta \hat{c}$ as a percentage of the full speed $c_0 + \Delta c$. The results show an error of less than 1% and confirm a good performance of the proposed algorithm. In the case of wind speed reconstruction, the true wind speed is given by the constant speed of $v = 7m/s$. The difference between the true value and reconstruction is shown in Fig.4. The arrows represent the wind vector direction at the tessellation grid points. We also found that the maximum difference in the amplitude is $\Delta v = 0.25 m/s$, which corresponds to an error of 3.5%. The algorithm converges after only 5 iterations.

6. CONCLUSIONS

The goal of this paper has been to present a new technique for the reconstruction of superposed two-dimensional temperature and wind flow fields, in the framework of acoustic tomography. In particular, we have shown that the transversal component of the resulting field can be deduced from the angle of arrival of the sound ray. The suggested iterative algorithm shows a good performance in terms of estimation accuracy and fast convergency. We are currently building a laboratory experiment to reconstruct actual flow and temperature fields from ultrasound tomographic measurements (with the parameters presented in Section 4) to experimentally validate the above simulations.

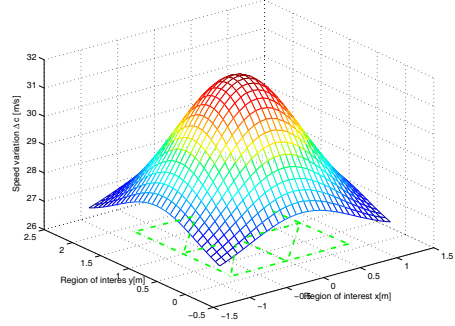


Fig. 2. True variation of sound speed Δc over the region of interest.

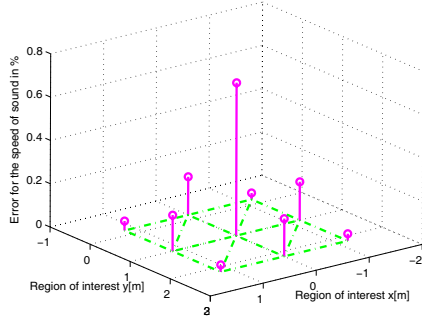


Fig. 3. Error in sound speed reconstruction, computed at the nodes of the tessellation grid.

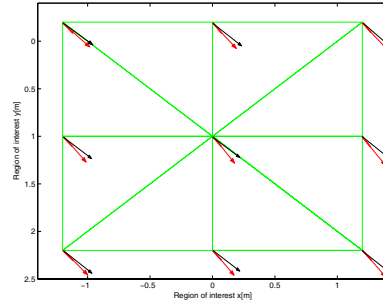


Fig. 4. The reconstructed and the true wind field computed at the nodes of the tessellation grid

7. REFERENCES

- [1] S. A. Johnson, J. F. Greenleaf, C. R. Hansen, W. F. Samayoa, A. Lent M. Tanaka, D. A. Christensen, and R. L. Wooley, "Reconstructing three-dimensional fluid velocity vector fields from acoustic transmission measurements," *Acoustical Holography*, L. W. Kessler, ed. New York: Plenum, vol. 7, pp. 307–326, 1977.
- [2] H. Braun and A. Hauck, "Tomographic reconstruction of vector fields," *IEEE Transactions on Signal Processing*, vol. 39, no. 2, 1991.
- [3] L. Sbaiz and M. Vetterli, "Acoustic flow tomography," Technical Report, LCAV/EPFL, 2003.
- [4] V. E. Ostashev, *Acoustics in moving inhomogeneous media*, E and FN SPON, London, 1997.
- [5] P. M. Woodward, *Probability and information theory, with applications to radar*, London : Pergamon Press, 1953.